Published in: Journal of Controlled Release (2007), vol.118, iss.3, pp.294-302
Status: Postprint (Author's version)

Helodermin-loaded nanoparticles: Characterization and transport across an in vitro model of the follicle-associated epithelium

Anne des Rieux[a,b], Virginie Fievez[a,b], Maryam Momtaz[c], Christophe Detrembleur[d], Maria Alonso-Sande[e], Jan Van Gelder[f], Annick Cauvin[f], Yves-Jacques Schneider[b], Véronique Préat[a]

[a] *Unité de Pharmacie Galénique, Université catholique de Louvain, Avenue E. Mounier, 73-20, 1200 Brussels, Belgium*
[b] *Laboratoire de Biochimie cellulaire, Institut des Sciences de la Vie, Université catholique de Louvain, Croix du Sud, 5, 1348 Louvain-La-Neuve, Belgium*
[c] *Laboratoire de Chimie Médicinale, Université catholique de Louvain, Place L. Pasteur, 1, 1348 Louvain-La-Neuve, Belgium*
[d] *Centre d'Etude et de Recherche sur les Macromolécules, Université de Liège, Sart-Tilman, 4000 Liège, Belgium*
[e] *Department of Pharmaceutical Technology, University of Santiago de Compostela, Santiago de Compostela, Spain*
[f] *Lilly Development Center, Parc Scientifique de Louvain-La-Neuve, Rue Granbonpré 11, 1348 Mont-Saint-Guibert, Belgium*

Abstract

M cells represent a potential portal for oral delivery of peptides and proteins due to their high endocytosis abilities. An *in vitro* model of human FAE (co-cultures) was used to evaluate the influence of M cells on the transport of free and encapsulated helodermin - a model peptide - across the intestinal epithelium. M cells enhanced transport of intact helodermin (18-fold, Papp = 3×10^{-6} cm s^{-1}). As pegylation increased nanoparticle transport by M cells, helodermin was encapsulated in 200 nm nanoparticles containing PEG-b-PLA:PLGA 1:1. Stability of the selected formulation was demonstrated in simulated gastric and intestinal fluids. M cells increased the transport of helodermin encapsulated in these nanoparticles by a factor of 415, as compared to Caco-2 cells. Transport of free and encapsulated helodermin occurred most probably by endocytosis. In conclusion, M cells improved helodermin transport across the intestinal epithelium, confirming their high potential for oral delivery of peptides.

Keywords: Peptide; M cells; *In vitro* model of the human follicle-associated epithelium (FAE); Polymeric nanoparticles; Oral delivery; Helodermin

1. Introduction

M cells are antigen and particle sampling cells, which are constitutive to the follicle-associated epithelium (FAE) as a part of Peyer's patches (PP) [1]. These cells have high transcytosis capabilities and are able to transport a broad range of materials, such as bacteria and viruses from the intestinal lumen to the underlying lymphoid tissues [2,3]. They represent then a potential portal for nanoparticles encapsulating vaccines or therapeutic peptides. Since M cells cannot be isolated and grown *in vitro*, an inverted *in vitro* model of the human FAE, a co-culture of Caco-2 cells and Raji cells [4], was employed to study M cell influence on transport of free peptide and nanoparticles containing the peptide through the intestinal mucosa.

It is widely known that, even if the oral route is the most convenient way to deliver peptide drugs or vaccines, the presence of highly active enzymes in the gastrointestinal tract as well as the low permeability of the intestinal epithelium lead to a very low bioavailability of orally administrated peptides. One commonly used strategy to bypass the early degradation of therapeutic peptides is to protect them by encapsulation in biocompatible and biodegradable nanoparticles [5]. Polymeric nanoparticles are solid colloidal carriers ranging in size from 10 to 1000 nm [6]. Different materials can be used to form these nanoparticles (lipids, polymers, natural biopolymers...), but poly(lactic) and poly(glycolic) acids have been extensively used as FDA approved biodegradable and biocompatible materials [7]. Moreover, nanoparticles should have the following properties for optimal oral delivery of peptide by M cells: (i) nanoparticles size in the range of 200 nm because nanoparticle transport by M cells is size dependent and the optimal size is about 200 nm [8-10]; (ii) stability in the gastrointestinal tract; (iii) long-circulating time of nanoparticles in the bloodstream; and (iv) absence of burst effect. Pegylation of nanoparticles is known to dramatically decrease plasmatic protein adsorption at the nanoparticle surface [11] and therefore recognition and capture by the mononuclear phagocyte system [12], as well as degradation and enzyme induced aggregation [13]. Stabilization in intestinal fluids has been reported [14]. However, PEG influence on nanoparticle transport by M cells has not been addressed.

To study M cell influence on the transport of peptides across the intestinal mucosa, helodermin was selected as a model peptide. This 35 amino acid residue linear peptide isolated from the venom of the lizard *Heloderma suspectum* [15] has a structure close to secretin and vasoactive intestinal polypeptide (VIP) and then share the same biological and pharmacological actions in many biological systems [16]. Helodermin, compared to VIP, shows a prolonged effect in many cells systems [17]. This could result from its C-terminal domain, that may protect the compound from enzymatic degradation, but could also contribute to the receptor binding [17].

Thus, prior to selection of the optimal formulation to encapsulate helodermin, transport by M cells of pegylated PLA/PLGA nanoparticles was compared to transport of PLGA nanoparticles using an *in vitro* model of human FAE. Next, a suitable method for helodermin nanoencapsulation was developed by assessing the influence of size, zeta potential, encapsulation efficiency and percentages of PEG exposed at the nanoparticle surface. Finally, M cell influence on the transepithelial transport of free helodermin and helodermin encapsulated in nanoparticles was studied using the *in vitro* FAE model.

2. Materials and methods

2.1. Materials

2.1.1. Chemicals

DL-Lactide (98%) was purchased from PURAC, recrystallized three times in toluene and dried under high vacuum at room temperature for 24 h before use. Polyethylene glycol 5000 monomethyl ether PEG (Mn, NMR=4,600 g/mol) was obtained from Fluka and stannous octoate from Sigma. Poly(lactide-co-glycolide) (Mw 40,000-70,000 g/mol), sodium acetate trihydrate, sodium cholic acid, boric acid, borax and sodium borohydide were purchased from Sigma. Poly(lactic-glycolic acid) Resomer RG 503 (PLGA 1:1, Mw 35,000 g/mol) was purchased from Boehringer Ingelheim. Helodermin was purchased from Bachem. Analytical grade acetic acid, dichloromethane, acetone, formaldehyde and sodium hydroxide were from Merck. D_20 and $CDCl_3$ were obtained from Sigma. Sodium boro[^{3}H]hydride (5 mCi) and autoradiography films (Hyperfilm) were supplied by Amersham Biosciences. Tris-Tricine running buffer (100 mM Tris, pH 8.3, 100 mM Tricine, 0.1% (w/v) SDS) was purchased from BioRad. Float-A-Lyzer® ready-to-use dialysis tube (Spectra/Por® Biotech Cellulose Ester membrane, cut off 1,000 g/mol, volume 1 ml) was purchased from Spectrum laboratories. Aqualuma came from Perkin Elmer and the micro-BCA kit was from Pierce. Acetonitrile was obtained from Acros Organics. Tetrhydrofuran (HPLC grade) was purchased from Biosolve. Yellow-green carboxylated latex particles (Fluo-Spheres®) with mean diameter of 0.2 µm were obtained from Molecular Probes.

2.1.2. Cell lines, cell culture media

Human colon carcinoma Caco-2 line (clone 1), obtained from Dr. Maria Rescigno, University of Milano-Bicocca, Milano (IT) [18], from passage x +12 to x +30, and human Burkitt's lymphoma Raji B line (American Type Culture Collection) from passage 102 to 110 were used.

Dulbecco modified Eagle's minimal essential medium (DMEM, 25 mM glucose), RPMI 1640 medium, non-essential amino acids, L-glutamine and penicillin-streptomycin (PEST) were purchased from Gibco™ Invitrogen Corporation. Heat inactivated fetal calf serum was from Hyclone (Perbio Sciences). Trypsin-EDTA consisted in 2.5% (w/v) of trypsin (Gibco™) and 0.2% (w/v) EDTA (IGN) in PBS (Gibco™). Hanks' balanced salt solution buffer (HBSS, pH 7.4), PBS with and without calcium and magnesium were obtained from Gibco™. Rhodamine-phalloidin was obtained from Molecular Probes. Glutaraldehyde was purchased from Merck. Transwell® polycarbonate inserts (12 wells, pore diameter of 3 µm, polycarbonate) were purchased from Corning Costar. Inserts were coated with Matrigel™ Basement Membrane Matrix (Becton Dickinson). Silicon tube (internal Ø 14 mm) was from Labo-Moderne. Petri dishes (glass, Ø x h (mm) = 200 x 50) were purchased from VWR.

2.2. Methods

2.2.1. Synthesis and characterization of PEG(4.6 K)-b-PLA (11 K) block copolymer

PEG-b-PLA was synthesized as previously described [19] by a conventional ring-opening polymerization of lactide initiated by a monohydroxy polyethylene glycol (Mn = 4600) at 114 °C for 4 h using tin octoate ($Sn(Oct)_2$) as catalyst until complete monomer conversion. The molecular weight of the PEG macroinitiator was increased to 21,600 g/mol and the polydispersity remained narrow (Mw/Mn = 1.15), in agreement with the

formation of a well-defined PEG-b-PLA diblock copolymer. The molecular weight of the first block (PEG) and second block (PLA) was 4,600 g/mol and 11,000 g/mol, respectively.

2.2.2. [^{3}H] radiolabeling of helodermin

Radiolabeling of helodermin was performed by reductive alkylation of amino groups as previously described [20]. The specific activity of [^{3}H] helodermin was obtained by measuring the total protein concentration by microBCA test, according to the manufacturer's instructions, and the radioactivity by liquid scintillation. [^{3}H] helodermin integrity was checked by RP-HPLC simultaneously with UV (retention time= 16.8 min as for unlabeled helodermin) and radioactivity (retention time = 17.3 min) detectors. Peptide integrity following labeling was also checked by autoradiography after SDS-PAGE electrophoresis (18% (w/v) of polyacrylamide gel, Tris-Tricine running buffer, data not shown). The specific activity of the peptide was 0.16 µCi/µg.

2.2.3. RP-HPLC analysis of helodermin

RP-HPLC system was from Waters and the solid phase was a C-18 column CC 125/4.6 Nucleosil® column (120-3, C18) and CC 8/4 Nucleosil® (120-3, C18) pre-column. The mobile phase consisted of an acetonitrile (ACN)/water gradient (25% to 60%; v/v (30 min); 1 ml/min, 50 µl injected), containing 0.01 M HC1. Detection was realized by UV (210 nm) (Waters) and radioactivity (Perkin Elmer) detectors. The limits of quantification of helodermin were 4 µg/ml and 54 µg/ml for UV and radioactivity detection, respectively.

2.2.4. Preparation of nanoparticles

PLGA nanoparticles were obtained by the simple emulsion method. PEG-b-PLA:PLGA nanoparticles were prepared by the double emulsion or by nanoprecipitation techniques [21]. Either empty, fluorescent, helodermin-loaded or fluorescent helodermin-loaded nanoparticles were prepared in function of the experimental requirements. When coumarin was incorporated at the same time as helodermin, we checked that the dye incorporation did not modify the characteristics of helodermin-loaded nanoparticles (size and zeta potential measurements).

Fluorescent PLGA nanoparticles were obtained by encapsulation of a fluorescent marker Rhodamine 6G (Sigma) by the simple emulsion method. Briefly, 20 µl of rhodamine 6G (2.5 mg/ml in ethanol) were added to 0.5 ml of a PLGA solution (50 mg/ml in dichloromethane) and emulsified by sonication (15 s, 20 W) into a 2-ml aqueous sodium cholate solution (1% w/v). This emulsion was diluted in 25 ml of sodium cholate solution (1%; w/v) and the solvent was evaporated. Finally, these nanoparticles were isolated at 10,000 g for 25 min and washed twice with water.

PEG-b-PLA:PLGA nanoparticles were prepared using the double emulsion technique, as described elsewhere [13]. Briefly, 50 µl of PBS or helodermin solution (50 or 100 µg) was added to 50 mg of polymer (25 mg of PEG-b-PLA, 25 mg of PLGA, unless stated otherwise) dissolved in 1 ml of dichloromethane. The solution was emulsified by sonication (15 s, 70 W) on ice. Then, 2 ml of a cold 1% (w/v) aqueous sodium cholate solution was added to this first emulsion (w/o) and the resulting emulsion (w/o/w) was formed by sonication (15 s, 70 W) on ice. The resulting double emulsion was diluted in 100 ml of a 0.3% (w/v) aqueous sodium cholate solution incubated at 37 °C. The organic solvent was eliminated under magnetic stirring, at 37 °C, according to Freitas et al. [22] who observed that protein encapsulation, as well as burst release, were influenced by the temperature during the sonication and solvent extraction/ evaporation phases. 6-Coumarin-loaded nanoparticles were prepared with the same procedure except that 0.2% (w/v) of 6-coumarin was added to the dichloromethane solution before primary emulsification [23], PEG-b-PLA:PLGA nanoparticles were also prepared by nanoprecipitation as previously described [24]. Briefly, 50 µl of PBS or helodermin solution (50 µg) and 100 mg of polymer (50 mg of PEG-b-PLA, 50 mg of PLGA) were dissolved in 5 ml of acetone. This organic solution was added dropwise to 10 ml deionized water under magnetic stirring and the solvent was removed at room temperature. Finally, the nanoparticles prepared by both methods were isolated by centrifugation (20,000x*g*-, 60 min) and washed three times in PBS.

For the determination of the encapsulation efficiency, the above-described formulations were prepared by incorporating [^{3}H] helodermin (50 µg, 8 µCi, unless stated). Fluorescent PEG-b-PLA:PLGA nanoparticles were obtained by addition of coumarin as described above.

2.2.5. Characterization of nanoparticles

Size and size distribution of nanoparticles were determined in water, at 37 °C, by DLS technique (Zetasizer Nano Series, Malvern) at 25 °C. Zeta potential *(ζ)* of nanoparticles was measured by Mixed mode measurement (M3) (Zetasizer Nano Series) at 25 °C in water.

Encapsulation efficiency was calculated from the amount of encapsulated [^{3}H] helodermin divided by the total amount of [^{3}H] helodermin recovered in supernatant and nanoparticles. [^{3}H] helodermin was quantified by liquid scintillation counting (Liquid scintillation counter, Wallac 1410, Amersham Bioscience). We checked that helodermin was not adsorbed on containers. Provided that plastic tubes were used, the loss of helodermin was low (less than 10%).

Integrity of helodermin after encapsulation was assessed, after extraction from nanoparticles, by RP-HPLC and autoradiography. Encapsulated [^{3}H] helodermin was extracted by dissolving lyophilized nanoparticles in dichloromethane and separating the peptide from the polymer by a liquid/liquid extraction (dichloromethane/water). Dichloromethane was then removed and the remaining aqueous phase was analyzed. In order to calculate PEG percentage exposed at the nanoparticle surface, ^{1}H-NMR analysis (Bruker AM 500 MHz) [14] was performed on nanoparticles suspended in D_2O or dissolved in $CDCL_3$. A known amount of sodium benzene -sulfonate was used as internal standard. It was then possible to quantify the molar concentration of PEG at the nanoparticle surface *vs.* the total molar concentration of PEG employed in the formulation.

2.2.6. In vitro stability studies

[^{3}H] helodermin-loaded nanoparticles (50 mg) were prepared accordingly to the procedure indicated above, centrifuged and redispersed in 1 ml PBS (pH 7.4). In order to assess the stability of the formulation, nanoparticles were incubated in different solutions: 50 µl of nanoparticle suspension was diluted in 500 µl of PBS, FaSSIF (Fasted State Simulated Intestinal Fluid: Sodium taurocholate 3 mM, lecithin 0.75 mM, NaOH 0.174 g, NaH2P04.H20 1.977 g, NaCl 3.093 g, purified water qs. 500 mL, pH 6.5.) [25], 0.1 M HC1, or in human plasma, and incubated at 37 °C under gentle shaking. After different durations, samples were taken out and centrifuged (15,000x*g*, 60 min). [^{3}H] helodermin release was assayed in supernatants by liquid scintillation. Samples of nanoparticles were centrifuged, freeze-dried and polymer molecular weights were analyzed by gel permeation chromatography (GPC).

2.2.7. Transport of helodermin, free and encapsulated, by M cells

2.2.7.1. Inverted in vitro model of the human FAE.

Caco-2 cells and Raji cells were grown as previously described [4,8,26], The inverted *in vitro* model of human FAE was obtained as described by des Rieux *et al.* [4]. Briefly, 3-5 days after Caco-2 cell seeding, inserts were inverted, placed in Petri dishes filled with supplemented DMEM+1% (v/v) PEST and a piece of silicon tube was placed on each insert basolateral side. Inverted cells were cultivated for 9-11 days and the basolateral medium was changed every other day. Then, Raji cells were added in insert basolateral compartments. Co-cultures were maintained for 5 days. Mono-cultures of Caco-2 cells, cultivated as above except for the presence of Raji cells, were used as controls. Prior to starting experiments, silicon tubes were removed; cell monolayers were placed in multiwell plates and washed twice in HBSS. Cell monolayer integrity, both in co- and monocultures, was controlled by transepithelial electrical resistance (TEER) measurement [4,8].

2.2.7.2. Transport experiments.

Free [^{3}H] helodermin was diluted in HBSS (1.6 µCi, 10 µg/ml) and was added to cell monolayer apical sides (400 µl). Cell monolayers were incubated for 60 min. at 37 °C (unless stated otherwise). Then, basolateral solutions were sampled and the amount of transported [^{3}H] labeled material was measured by liquid scintillation. Integrity of transported free [^{3}H] helodermin was checked by RP-HPLC performed on pooled samples.

Since transport of 0.2 µm carboxylated polystyrene nanoparticles (model nanoparticles) has been well characterized [4,8,26], these nanoparticles were used as control of the *in vitro* model functionality. Concentrations of fluorescent carboxylated, pegylated (PEG-b-PLA:PLGA nanoparticles) and PLGA nanoparticles were adjusted from stock solutions (checked by FACS analysis) by dilution in HBSS, to a final concentration of 4.5×10^9, 4×10^{10} and 6×10^7 nanoparticles/ml, respectively, and vortexed for 1 min to dissociate possible aggregates. After equilibration in HBSS at 37 °C (unless stated), apical medium of cell

monolayers was replaced by nanoparticle suspension (400 µl) and cell monolayers were incubated at 37 °C (unless stated) for 60 min. Then, basolateral solutions were sampled and the number of transported nanoparticles was measured using a flow cytometer (FACScan, Becton Dickinson) [8,26]. Results are expressed as apparent permeability coefficient (Papp), as a mean ± standard error of the mean (SEM).

2.2.7.3. Localization of nanoparticles in cell monolayers.

After transport experiments, cells were fixed on ice in 4% (v/v) buffered formaldehyde (pH 7.4, 10 min) and washed twice in 500 µl cold HBSS. Actin was stained with 250 µl of rhodamine-phalloidin (4 U/ml) in HBSS+0.2% (v/v) Triton X-100 for 10 min to reveal cell borders. Cells were washed in HBSS, cut and mounted on glass slides. Nanoparticle position in cell monolayer was observed with a DMIRE2 Leica™ confocal microscope. Data were analyzed by Leica confocal software to obtain *y—z* and *x—y* views of cell monolayers.

2.2.7.4. Cytotoxicity studies.

Caco-2 cells were cultivated on 96 well plates (0.33 cm per well) with a density of 3×10^4 cells per well for approximately 3 days. Cytotoxicity studies were performed for PLGA and PEG-b-PLA:PLGA nanoparticles at concentrations between 0.05 and 5 mg/ml (0.1 ml/well). Incubation duration was fixed at 90 min. Then nanoparticle suspensions were removed and cell viability was measured by using the colorimetric MTT assay [27].

2.2.7.5. Statistics.

Differences between treated groups were analyzed using Mann-Whitney non-parametric test ($n \geq 3$, significance $P<0.05$).

3. Results

3.1. Influence of PEG at the nanoparticle surface on their transport by M cells

In order to determine whether PEG chain presence at the nanoparticle surface could influence their uptake and transport by M cells, the transport of fluorescent PLGA and PEG-b-PLA: PLGA (1:1, w/w) nanoparticle was compared in an inverted *in vitro* model of human FAE [4]. While their sizes were similar (219 ± 21 and 194 ± 2 nm, respectively), zeta potentials decreased from -20 ± 9 to -4 ± 5 mV in HBSS. The incubation of PEG-b-PLA:PLGA and PLGA nanoparticles with Caco-2 monolayers did not affect cell viability (MTT assay) up to 5 mg of nanoparticles/cm^2 (data not shown).

Mono- and co-cultures were incubated with nanoparticle suspensions at 37 °C, and Papp of non-pegylated and pegylated nanoparticles were compared. The functionality of the inverted FAE *in vitro* model was first confirmed by a 600 times higher transport of model nanoparticles by co-cultures compared to mono-cultures ($2.2 \times 10^{-8} \pm 7.9 \times 10^{-9}$ $cm.s^{-1}$ and $3.5 \times 10^{-11} \pm 1.1 \times 10^{-11}$ $cm.s^{-1}$, respectively). PEG-b-PLA:PLGA and PLGA nanoparticles were more transported by co-cultures than by monocultures (Fig. 1). The co-cultures/mono-cultures ratio was much higher for PEG-b-PLA:PLGA nanoparticles than for PLGA nanoparticles (400 and 2, respectively). This could be explained by a combination of a 2-fold more efficient transport of pegylated nanoparticles by the co-cultures ($P<0.05$) with a 120-fold higher transport of PLGA nanoparticles by mono-cultures as compared to pegylated nanoparticles ($P<0.05$).

3.2. Formulation of nanoparticles for helodermin encapsulation

3.2.1. Formulation and physicochemical characterization

Nanoparticle size in the range of 200 nm is optimal for their uptake and transport by M cells [8]. In addition, PEG chains at the nanoparticle surface increase their uptake by M cells (Fig. 1). Hence, helodermin was encapsulated in 200 nm pegylated biodegradable nanoparticles.

Two techniques can be used to encapsulate a peptide in PLGA-based nanoparticles. Nanoprecipitation is adapted to hydrophobic molecules, whereas double emulsion was developed to encapsulate hydrophilic molecules. Since helodermin is amphiphilic, the two methods were compared.

Zeta potentials, sizes of nanoparticles and encapsulation efficiency were similar whatever the preparation method

used (Table 1). Total removal of surfactant (cholic acid) from nanoparticle suspensions was confirmed by ^{1}H NMR analysis (data not shown). Addition of helodermin did not change nanoparticle properties. However, a higher percentage of PEG at the nanoparticle surface and a lower polymer mass loss after formulation were observed for nanoparticles produced by double emulsion. Thus, the double emulsion method was chosen to encapsulate helodermin.

Fig. 1: *Influence of PEG chains exposed at nanoparticle surface on their transport by M cells. Transport experiments were run in HBSS. Fluorescent PLGA or PEG-b-PLA:PLGA nanoparticles were added apically and incubated for 60 min at 37 °C with mono- and co-cultures. In this experiment no helodermin was encapsulated in nanoparticles (n=4). (a) P<0.05 versus pegylated nanoparticles; (b) P<0.05 versus mono-cultures.*

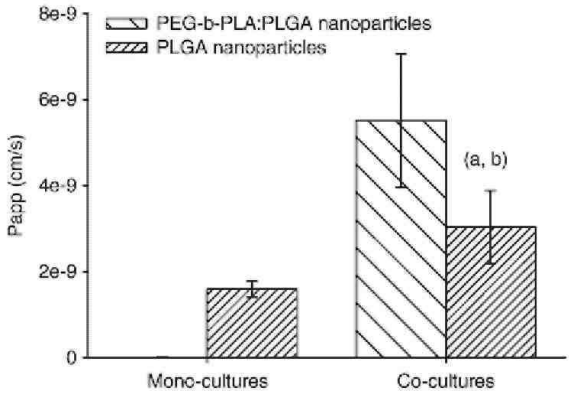

Table 1: *Encapsulation of helodermin by nanoprecipitation and by double emulsion: comparison of different formulation parameters*

	Nanoprecipitation		**Double emulsion**		
	Unloaded	**Helodermin loaded**	**Unloaded**	**Helodermin loaded**	**Helodermin loaded**
Initial polymer mass (mg)	100	100	50	50	50
Amount of helodermin (µg)		50		50	100
Polymer mass loss after formulation	51 ± 11	NA	9.5 ± 6	NA	NA
Size(nm)[a,b]	138 ± 2	133 ± 13	194 ± 16	180 ± 5	196 ± 2.3
PDI	0.164	0.137	0.194	0.159	0.159
Zeta potential (mV)[a,b]	-20 ± 3	-17 ± 2	-4 ± 5	-16 ± 11	-13 ± 11
Encapsulation efficiency	NA[c]	42 ± 2	NA	42 ± 3	26 ± 8
PEG exposed at nanoparticle surface (%)	41	NA	59	NA	NA

A blend of PEG-b-PLA and PLGA was used (ratio 1:1 (w/w)) to formulate nanoparticles.
[a] Values are mean for duplicates (polymer loss) and mean ± SD for triplicates (particle size, zeta potential and encapsulation efficiency).
[b] Measures were performed in milliQ water.
[c] Not assayed.

The optimal proportion of PLGA and PEG-b-PLA polymers in the formulation was then determined. As summarized in Fig. 2, PEG-b-PLA:PLGA ratio influenced nanoparticle size, zeta potential and PEG percentage at their surface. Nanoparticle size increased slightly with PEG-b-PLA concentration up to a 1:1 ratio, from 125 nm to 195 nm, and then stabilized. Zeta potential increased also with PEG-b-PLA concentration up to a 1:1 ratio, from -60 mV to -20 mV, and then decreased to -40 mV when the formulation was composed of 75% and 100% of PEG-b-PLA. The percentage of PEG at nanoparticle surface increased with the percentage of PEG-b-PLA in the formulation. It reached a maximum when 50% of the formulation was composed of PLA-PEG In conclusion,

all the tested formulations provided nanoparticles with a diameter of about 200 nm, but nanoparticles prepared with a 1:1 ratio presented the highest amount of PEG chains at their surface.

[^{3}H] helodermin integrity was demonstrated after encapsulation, extraction and analysis by RP-HPLC (data not shown). When the amount of [^{3}H] peptide was doubled, size and zeta potential were similar, in contrast to encapsulation efficiency (Table 1). However, even if encapsulation efficiency was lower for 100 µg of helodermin added in the formulation, the total amount of encapsulated peptide was similar (25.5 ± 2.5 µg and 26 ± 7.4 µg, for 100 µg and 50 µg incorporated, respectively). These results were confirmed by a micro BCA test (data not shown).

3.2.2. In vitro stability studies

To evaluate their stability, helodermin-loaded PEG-b-PLA: PLGA (1:1 (w/w)) nanoparticles were incubated in PBS (pH 7.4, 21 days), in simulated gastric medium (0.1 M HCl,2 h) (European Pharmacopoeia), in simulated intestinal fluid (FaSSIF, 24 h) [25] and in human plasma (48 h).

Polymer degradation was evaluated after incubation of nanoparticles in PBS and in 0.1 M HC1 by gel permeation chromatography (GPC). The relative Mw (polystyrene standard curve) decreased upon 2 days of nanoparticle incubation in PBS, but not significantly upon 2 h of incubation in 0.1 M HC1 (Fig. 3). Additionally, the mean sizes of nanoparticles, whatever the medium or duration of incubation, remained unchanged during stability studies (Fig. 4). The [^{3}H] helodermin release remained low (< 5%) in PBS and human serum, but was higher in FaSSIF and 0.1 M HC1 (<25%). In FaSSIF and HC1, helodermin release could be explained by the detachment of adsorbed helodermin at nanoparticle surface. Since the nanoparticle size remained unchanged, the nanoparticle degradation would probably not be responsible for the helodermin release. After a first rapid desorption phase, the release increased quite slowly (10% in 2 h). Finally, the integrity of released helodermin after 2 h in 0.1 M HCL and 24 h in PBS or FaSSIF was controlled by RP-HPLC (data not shown).

In conclusion, the obtained nanoparticles had an acceptable stability in various media. Therefore, this formulation can be considered as suitable for oral administration.

Fig. 2: *Influence of PEG-b-PLA percentage in the formulation on nanoparticle size, zeta potential and PEG percentage at the nanoparticle surface. Size and zeta potential measurements were realized in milliQ water, whereas PEG percentage at the nanoparticle surface was evaluated by ^{1}H RMN in D_2O (n = 3).*

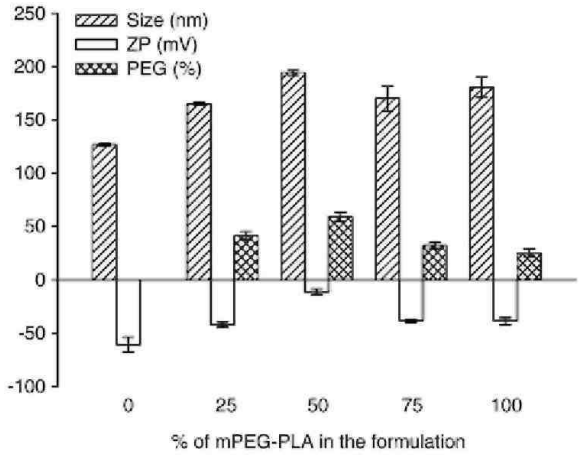

Fig. 3: *Stability study of nanoparticles consisting of 1:1 (w/w) PEG-b-PLA: PLGA, produced by double emulsion, evaluated by measuring polymer molecular weights by GPC. Nanoparticles were incubated for 56 days in PBS at 37 °C or incubated for 2 h in 0.1 M HCl at 37 °C (simulated gastric fluid) (n=2).*

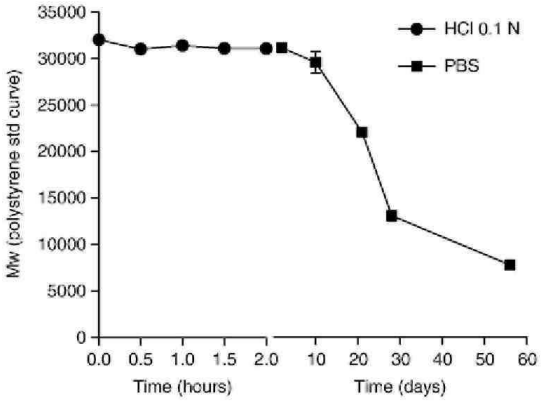

Fig. 4: *Stability study of nanoparticles (1:1 (w/w) PEG-b-PLA:PLGA; 50 µg [^{3}H] helodermin incorporated in the formulations) evaluated following nanoparticle size (■) as well as [3H] helodermin release (♂). Nanoparticles were incubated at 37 °C, for 21 days in PBS (pH 7.4), for 2 h in 0.1 M HC1 (simulated gastric fluid), 24 h in FaSSIF (fasted state simulated intestinal fluid, pH 6.5), or 24 h in human serum (n = 3).*

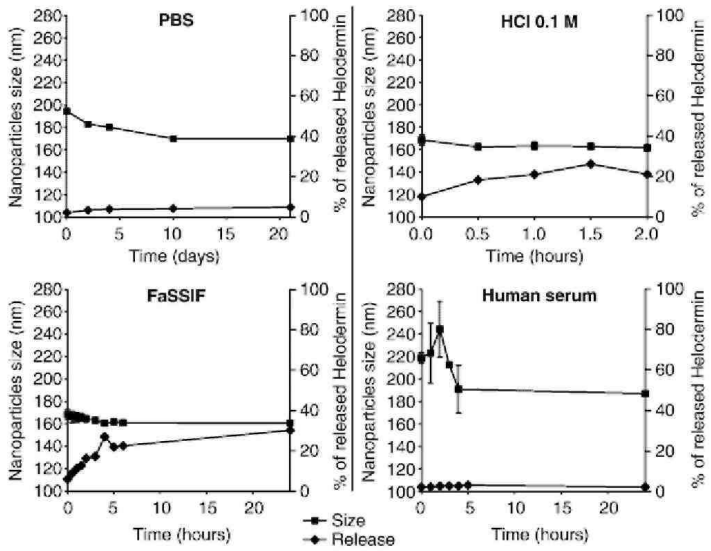

3.3. Influence of M cells on helodermin transport across the intestinal mucosa

3.3.1. Transport of free helodermin by M cells

Following incubation of [^{3}H] helodermin with mono- and co-cultures, radioactivity was detected at a 5-fold higher level in basolateral compartments of co-cultures compared to monocultures (Fig. 5A). However, RP-HPLC analysis of basolateral media underlined the degradation of 75% of [^{3}H] helodermin transported by mono-cultures, whereas [^{3}H] helodermin transported by co-cultures remained intact (Fig. 5A). M cell presence in the *in vitro* cell co-culture model resulted in a 18-fold increase in transport of intact helodermin in the basolateral compartment, compared to cell monolayers consisting exclusively of Caco-2 cells. In addition, helodermin transport by co-cultures was temperature dependent (Fig. 5B).

3.3.2. Transport of encapsulated helodermin by M cells Co-cultures transported helodermin-loaded nanoparticles

(PEG-b-PLA:PLGA nanoparticles) 415-fold more than monocultures, by a temperature-dependent process (Fig. 6A). The transport of carboxylated nanoparticles (model nanoparticles) confirmed the *in vitro* model of human FAE functionality (nanoparticle transport 620-fold higher by co-cultures compared to mono-cultures) and was also a positive control of transport inhibition at 4°C. Helodermin-loaded nanoparticle transport was 4 times lower compared to model nanoparticles (Fig. 6A).

Confocal microscopy allowed to localize helodermin-loaded nanoparticles within co-cultures [8] (Fig. 6B), thus confirming a transcellular transport of helodermin encapsulated in nanoparticles. These observations suggest that transport of helodermin-loaded nanoparticles by M cells could occur by endocytosis.

Fig. 5: *M cell influence on free helodermin transport. Transport experiments were run in HBSS on the in vitro model of human FAE. Free helodermin solutions were added apically to cell monolayers and incubated for 60 min. (A) Helodermin was incubated with mono- and co-cultures at 37 °C. Papp were evaluated by measuring radioactivity in basolateral compartments and helodermin integrity was evaluated by RP-HPLC (n=4). (a) P<0.05 versus total helodermin transported by mono-cultures; (b) P<0.05 versus monocultures. (B) Temperature influence on free helodermin transport. Helodermin transport across co-culture monolayers was evaluated at 4 and 37 °C (n=4). Papp measured on mono-cultures were not significantly different at 4 and 37 °C (data not shown), (a) P<0.05 versus 4 °C.*

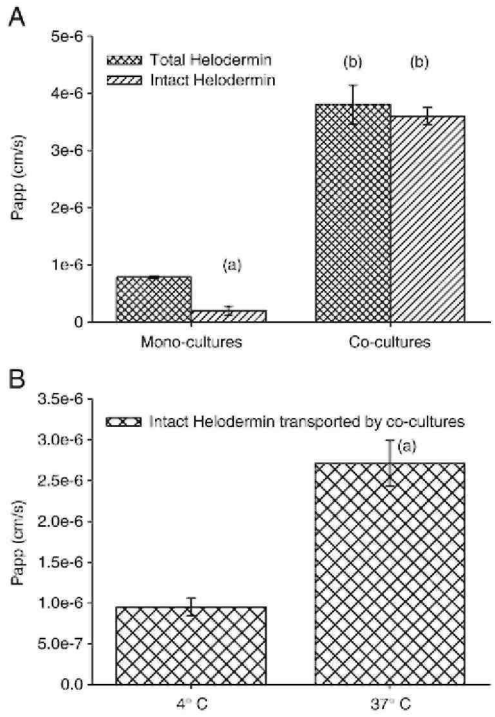

4. Discussion and conclusion

M cell influence on transport across the intestinal epithelium of a model peptide, helodermin, either free or encapsulated in nanoparticles, was studied using an *in vitro* model of the FAE [4], Transport experiments performed with this *in vitro* model indicated that: (i) free and encapsulated helodermin were more transported by M cells than by Caco-2 cells, although helodermin was 650 times more transported free than encapsulated across the *in vitro* model; (ii) free helodermin was not degraded during its transport by M cells, which was not the case upon incubation with enterocyte-like cells; (iii) pegylation of nanoparticles increased (2-fold) their transport by M cells compared to PLGA nanoparticles; and (iv) helodermin transport, free or encapsulated, is temperature dependent.

Fig. 6: *M cell influence on helodermin-loaded nanoparticle transport. (A) Temperature influence. Helodermin-loaded nanoparticle transport across co-culture monolayers was studied at 4 and 37 °C. Transport of model carboxylated nanoparticles assessed the functionality of the in vitro model and stand for a control of the transport inhibition at 4 °C (n=4). (a) P<0.05 versus carboxylated nanoparticles; (b) P<0.05 versus mono-cultures; (c) P<0.05 versus 4 °C; (d) P<0.05 versus carboxylated nanoparticles. (B) Localization of helodermin-loaded nanoparticles in cell monolayers. Cells were stained with rhodamine-phalloidin (red) and nanoparticles were labeled with coumarin (yellow-green). Mono (a, b)- and co-cultures (c, d) were fixed and stained after incubation with yellow-green helodermin-loaded nanoparticles at 37 °C during 60 min. Mono-cultures were used as controls. Lines indicate where, within the cell monolayers, pictures were taken and analyzed. Circles indicate nanoparticle localization in cell monolayers.*

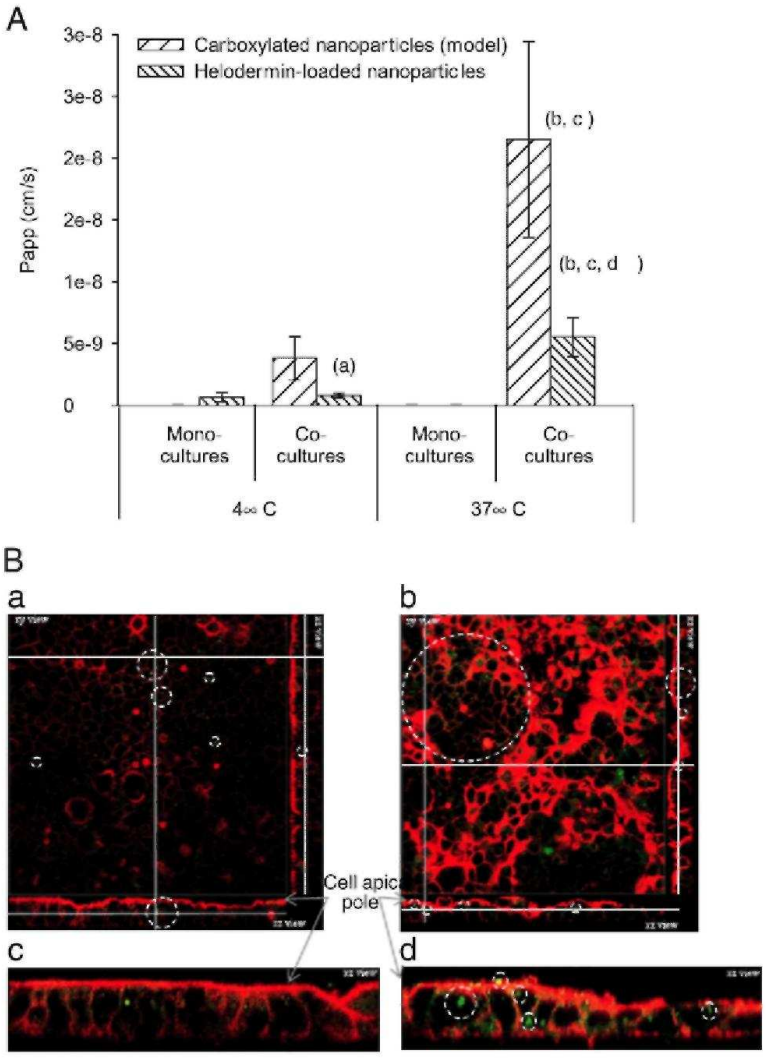

4.1. Transport of free helodermin by M cells

For the first time, it has been demonstrated, using an *in vitro* model of the human FAE, that M cells were able to deliver an intact peptide at their basolateral pole, and that the transport of free non-degraded helodermin was enhanced by a factor of 20 in the presence of M cells as compared to Caco-2 cells. This is not totally surprising considering that M cells have been known to conduct transport of intact macromolecules from one side of the barrier to the other [28]. Besides a reduced number of lysosomes [1,29], lower levels of membrane-associated hydrolases [30] might allow antigens to remain intact in these regions of the epithelial surface [31]. Transport of intact protein has already been suggested by Liang *et al.* [32] who demonstrated the ability of ovalbumin to elicit *in vitro* an immune response after its transport by M cells of an *in vitro* model. However, they did not assess ovalbumin integrity after its transport. Compared to 4 kDa Dextran [4], a hydrophilic molecule that pass through M cell-Caco-2 monolayers by the paracellular route, helodermin was 14-fold more transported by co-cultures. This could be explained by a higher hydrophobicity of helodermin, reducing the paracellular contribution to

transepithelial transport, while favoring its transport by the transcellular route. Further studies should be performed to confirm this hypothesis.

4.2. Influence of pegylation on nanoparticle transport by M cells

To orally deliver helodermin, a nanoparticle formulation was developed to protect peptides from degradation in the GI tract and to enhance uptake by intestinal M cells. Previous studies have shown that the optimal nanoparticle size for M cell delivery was about 200 nm [8-10]. The influence of nanoparticle surface properties on their uptake by M cell is well known but optimal properties, e.g., hydrophobicity, zeta potential, remain controversial. In particular, PEG influence on nanoparticle transport by M cells has not been described. We show that PLGA nanoparticle transport by M cells was higher when PEG chains were exposed at the nanoparticle surface. This was quite unexpected, since it was previously observed that hydrophobic nanoparticles were more transported by M cells than less hydrophobic ones [8,33]. However, this result is in agreement with some recent data that suggest that the presence of PEG on the surface of nanoparticles could increase their transport across mucosal surfaces. For instance, Alonso's group [13,14,34,35] observed that a hydrophilic PEG coating nanoparticles dramatically increased macromolecule bioavailability. In addition, PEG coating around nanoparticles make these nanoparticles more stable upon contact with physiological fluids. PEG chains could hinder protein/enzyme adsorption, thereby protecting nanoparticles against degradation and enzyme induced aggregation [13], However, it is not well defined whether the improvement of drug bioavailability was due to a greater stability of the formulation or whether the presence of PEG could play a role in facilitating nanoparticle transport. The reduced transport of pegylated nanoparticles by Caco-2 cells agrees with observations by Behrens *et al.* [36], describing almost no association of PLA-PEG nanoparticles with Caco-2 cells and a very low transport, which suggests therefore that PEG-chains could inhibit interactions with Caco-2 cell surface. However, pegylated nanoparticles were less transported than carboxylated polystyrene nanoparticles. The most probable origin is the influence of surface properties (zeta potential, charge density, hydrophobicity, etc.).

In conclusion, while the pegylation of nanoparticles improved their uptake by M cells, it reduced their transport by Caco-2 cells. Further studies would be required to understand by which mechanism(s) pegylation improved nanoparticle transport by M cells.

4.3. Influence of encapsulation on helodermin transport by M cells

In order to optimize the nanoparticle uptake by M cells, the formulations tested to encapsulate helodermin consisted of PEG-b-PLA and PLGA polymers. The nanoparticles were prepared by the double emulsion technique. They had a size about 200 nm, a neutral zeta potential and contained 0.42 µg of helodermin/mg of polymer.

As expected from previous studies, helodermin-loaded nanoparticle transport was 415 times higher in the presence of M cells. However, our data underline the much higher transport (650-fold) of free helodermin by M cells compared to helodermin-loaded nanoparticle transport. Why free helodermin was transported more effectively by M cells than the encapsulated one is not clear yet, but it could be hypothesized that M cell endocytosis mechanisms differ as a function of the material to be transcytosed. Anyway, further investigations would be required to determine the *in vivo* performance of free helodermin compared to encapsulated helodermin.

In conclusion, M cells improved the transport of helodermin, free and encapsulated, through an active phenomenon, most probably endocytosis.

Acknowledgments

The authors thank Dr. Perez-Morga from the Department of Molecular Biology, *Université libre de Bruxelles* for its scientific and technical support in the realization of confocal analysis as well as André Tonon from the Brussels Ludwig Institute Cancer Research for his support in the realization of FACScan analysis. Bernard Ucakar, from the School of Pharmacy, *Université catholique de Louvain*, is acknowledged for his technical support as well as Jean-Pierre Vandiest, from the School of Pharmacy, *Université catholique de Louvain*, for his help with the figures. Dr. Detrembleur thanks the « *Politique Scientifique Fédérale* » for financial support in the frame of the "Interuniversity Attraction Poles Programme (IUAP V/03): Supramolecular Chemistry and Supramolecular Catalysis". This work was supported by the *Région Wallonne* (DGTRE), First Europe (n°

215099 and 415847) and VACCINOR project (WINOMAT), by the *Fond Scientifique de Recherche* of the *Université catholique de Louvain* and the *Fonds National de la Recherche Scientifique* (Belgium).

References

[1] A. Gebert, H.J. Rothkotter, R. Pabst, M cells in Peyer's patches of the intestine, Int. Rev. Cyt. 167 (1996) 91-159.

[2] R.L. Owen, Uptake and transport of intestinal macromolecules and microorganisms by M cells in Peyer's patches—a personal and historical perspective, Semin. Immunol. 11 (3) (1999) 157-163.

[3] M.R. Neutra, Interactions of viruses and microparticles with apical plasma membranes of M cells: implications for human immunodeficiency virus transmission, J. Infect. Dis. 179 (Suppl 3) (1999) S441-S443.

[4] A. des Rieux, V. Fievez, I. Théate, J. Mast, V. Preat, YJ. Schneider, An improved in vitro model of the human intestinal follicle associated epithelium for studies of nanoparticles by M cells, Eur. J. Pharm. Sci. (in press).

[5] A. des Rieux, V. Fievez, M. Garinot, Y.J. Schneider, V. Preat, Nanoparticles as potential oral delivery systems of proteins and vaccines: a mechanistic approach, J. Control. Release 116 (1) (2006) 1-27.

[6] S.A. Galindo-Rodriguez, E. Allemann, H. Fessi, E. Doelker, Polymeric nanoparticles for oral delivery of drugs and vaccines: a critical evaluation of in vivo studies, Crit. Rev. Ther. Drug Carr. Syst. 22 (5) (2005) 419-464.

[7] M. Vert, Polyvalent polymeric drug carriers, Crit. Rev. Ther. Drug Carr. Syst. 2 (3) (1986) 291-327.

[8] A. des Rieux, E.G.E. Ragnarsson, E. Gullberg, V. Preat, Y.J. Schneider, P. Artursson, Transport of nanoparticles across an in vitro model of the human intestinal follicle associated epithelium, Eur. J. Pharm. Sci. 25 (4-5) (2005) 455-465.

[9] M.P. Desai, V. Labhasetwar, G.L. Amidon, R.J. Levy, Gastrointestinal uptake of biodegradable microparticles: effect of particle size, Pharm. Res. 13 (12) (1996) 1838-1845.

[10] S. McClean, E. Prosser, E. Meehan, D. O'Malley, N. Clarke, Z. Ramtoola, D. Brayden, Binding and uptake of biodegradable poly-DL-lactide micro- and nanoparticles in intestinal epithelia, Eur. J. Pharm. Sci. 6 (2) (1998) 153-163.

[11] V.C. Mosqueira, P. Legrand, A. Gulik, O. Bourdon, R. Gref, D. Labarre, G Barratt, Relationship between complement activation, cellular uptake and surface physicochemical aspects of novel PEG-modified nanocapsules, Biomaterials 22 (22) (2001) 2967-2979.

[12] H. Otsuka, Y Nagasaki, K. Kataoka, PEGylated nanoparticles for biological and pharmaceutical applications, Adv. Drug Deliv. Rev. 55 (3) (2003) 403-419.

[13] M. Tobio, A. Sanchez, A. Vila, I. Soriano, C. Evora, J.L. Vila-Jato, M.J. Alonso, The role of PEG on the stability in digestive fluids and in vivo fate of PEG-PLA nanoparticles following oral administration, Colloids Surf, B Biointerfaces 18 (3-4) (2000) 315-323.

[14] A. Vila, H. Gill, O. McCallion, M.J. Alonso, Transport of PLA-PEG particles across the nasal mucosa: effect of particle size and PEG coating density, J. Control. Release 98 (2) (2004) 231-244.

[15] M.C. Vandermeers-Piret, A. Vandermeers, P. Gourlet, M.H. Ali, M. Waelbroeck, P. Robberecht, Evidence that the lizard helospectin peptides are O-glycosylated, Eur. J. Biochem. 267 (14) (2000) 4556-4560.

[16] M. Hoshino, C. Yanaihara, Y.M. Hong, S. Kishida, Y Katsumaru, A. Vandermeers, M.C. Vandermeers-Piret, P. Robberecht, J. Christophe, N. Yanaihara, Primary structure of helodermin, a VIP-secretin-like peptide isolated from Gila monster venom, FEBS Lett. 178 (2) (1984) 233-239.

[17] W. Blankenfeldt, K. Nokihara, S. Naruse, U. Lessel, D. Schomburg, V. Wray, NMR spectroscopic evidence that helodermin, unlike other members of the secretin/VIP family of peptides, is substantially structured in water, Biochemistry 35 (19) (1996) 5955-5962.

[18] M. Rescigno, M. Urbano, B. Valzasina, M. Francolini, G Rotta, R. Bonasio, F. Granucci, J.P. Kraehenbuhl, P. Ricciardi-Castagnoli, Dendritic cells express tight junction proteins and penetrate gut epithelial monolayers to sample bacteria, Nat. Immunol. 2 (4) (2001) 361-367.

[19] R. Gref, M. Luck, P. Quellec, M. Marchand, E. Dellacherie, S. Harnisch, T. Blunk, R.H. Muller, 'Stealth' corona-core nanoparticles surface modified by polyethylene glycol (PEG): influences of the corona (PEG chain length and surface density) and of the core composition on phagocytic uptake and plasma protein adsorption, Colloids Surf. B Biointerfaces 18 (3-4) (2000) 301-313.

[20] G.E. Means, R.E. Feeney, Reductive alkylation of amino groups in proteins, Biochemistry 7 (6) (1968) 2192-2201.

[21] D. Bazile, C. Prud'homme, M.T. Bassoullet, M. Marlard, G. Spenlehauer, M. Veillard, Stealth Me.PEG-PLA nanoparticles avoid uptake by the mononuclear phagocytes system, J. Pharm. Sci. 84 (4) (1995) 493-498.

[22] S. Freitas, H.P. Merkle, B. Gander, Microencapsulation by solvent extraction/evaporation: reviewing the state of the art of microsphere preparation process technology, J. Control. Release 102 (2) (2005) 313-332.

[23] X. Gao, W. Tao, W. Lu, Q. Zhang, Y. Zhang, X. Jiang, S. Fu, Lectin-conjugated PEG-PLA nanoparticles: preparation and brain delivery after intranasal administration, Biomaterials 27 (18) (2006) 3482-3490.

[24] H. Fessi, F. Puisieux, J.P. Devissaguet, N. Ammoury, S. Benita, Nanocapsule formation by interfacial polymer deposition following solvent displacement, Int. J. Pharm. 55 (1) (1989) R1-R4.

[25] J.B. Dressman, C. Reppas, In vitro-in vivo correlations for lipophilic, poorly water-soluble drugs, Eur. J. Pharm. Sci. 11 (Suppl 2) (2000) S73-S80.

[26] E. Gullberg, M. Leonard, J. Karlsson, A.M. Hopkins, D. Brayden, A.W. Baird, P. Artursson, Expression of specific markers and particle transport in a new human intestinal M-cell model, Biochem. Biophys. Res. Commun. 279 (3) (2000) 808-813.

[27] L. Ould-Ouali, M. Noppe, X. Langlois, B. Willems, R.P. Te, P. Timmerman, M.E. Brewster, A. Arien, V. Preat, Self-assembling PEG-p (CL-co-TMC) copolymers for oral delivery of poorly water-soluble drugs: a case study with risperidone, J. Control. Release 102 (3) (2005) 657-668.

[28] M.R. Neutra, T.L. Phillips, E.L. Mayer, D.J. Fishkind, Transport of membrane-bound macromolecules by M cells in follicle-associated epithelium of rabbit Peyer's patch, Cell Tissue Res. 247 (3) (1987) 537-546.

[29] J. Mach, T. Hshieh, D. Hsieh, N. Grubbs, A. Chervonsky, Development of intestinal M cells, Immunol. Rev. 206 (1) (2005) 177-189.

[30] R.L. Owen, D.K. Bhalla, Cytochemical analysis of alkaline phosphatase and esterase activities and of lectin-binding and anionic sites in rat and mouse Peyer's patch M cells, Am. J. Anat. 168 (2) (1983) 199-212.

[31] J.P. Kraehenbuhl, M.R. Neutra, Epithelial M cells: differentiation and function, Annu. Rev. Cell Dev. Biol. 16 (1) (2000) 301-332.

[32] E. Liang, A.K. Kabcenell, J.R. Coleman, J. Robson, R. Ruffles, M. Yazdanian, Permeability measurement of macromolecules and assessment of mucosal antigen sampling using in vitro converted M cells, J. Pharmacol. Toxicol. Methods 46 (2) (2002) 93-101.

[33] J.H. Eldridge, C.J. Hammond, J.A Meulbroek, J.K. Staas, R.M. Gilley, T.R. Tice, Controlled vaccine release in the gut-associated lymphoid-tissues. 1. Orally-administered biodegradable microspheres target the Peyers patches, J. Control. Release 11 (1-3) (1990) 205-214.

[34] M. Tobio, R. Gref, A. Sanchez, R. Langer, M.J. Alonso, Stealth PLA-PEG nanoparticles as protein carriers for nasal administration, Pharm. Res. 15 (2) (1998) 270-275.

[35] A. Vila, A. Sanchez, M. Tobio, P. Calvo, M.J. Alonso, Design of biodegradable particles for protein delivery, J. Control. Release 78 (1-3) (2002) 15-24.

[36] I. Behrens, A.I. Pena, M.J. Alonso, T. Kissel, Comparative uptake studies of bioadhesive and non-bioadhesive nanoparticles in human intestinal cell lines and rats: the effect of mucus on particle adsorption and transport, Pharm. Res. 19 (8) (2002) 1185-1193.